MALAYSIAN JOURNAL OF SCIENCE
MJS
ISSN 1394-3065

Regular Issue

Malaysian Journal of Science 43 (4): 20-30 (December 2024) https://mjs.um.edu.my

Photocatalytic Degradation of Ethylene Bis-Dithiocarbamate Fungicide from Wastewater Using Cerium Oxide Nanoparticles under Natural Solar Irradiation

Mahadi Danjuma Sani[1ac]*, Abbaraju V.D.N. Kumar[2a] and Venugopal N.V.S.[3b]

Abstract: This study developed a suitable method for the degradation of ethylene bis-dithiocarbamate pesticide mancozeb in wastewater and agricultural runoff using nanoceria as photocatalysts. The nanoceria or cerium oxide nanoparticles were synthesized using a simple coprecipitation method with cerium nitrate hexahydrate ($Ce(NO_3)_3.6H_2O$) and Potassium carbonate (K_2CO_3) as a precursor and precipitating agent respectively. The synthesized powder particle was further ascertained through characterization using Scanning Electron Microscopy SEM for surface morphology, Fourier Transform Infrared Spectroscopy FTIR for the determination of the functional groups, Powder X-ray diffraction PXRD for crystal structure, phase and crystallite size and Energy Dispersive X-ray Spectroscopy EDAX for elemental composition of the synthesized nanoceria. It was revealed that the nanoparticle was successfully synthesized with a crystallite size of 27 nm. Photocatalytic degradation of mancozeb pesticide using the synthesized NPs was determined in batches with optimization of certain parameters including; the initial concentration of pesticide, quantity of the photocatalyst, irradiation time, calcination temperature and UV index. Nanoceria was found to degrade more than 62% of the initial concentration of mancozeb in 2 hours. Nanoceria usually acts as an active sorbent in the destruction of pesticides in wastewater and as such, its application on the degradation of mancozeb is crucial and significant. This method can be suitable for agricultural runoff and synthetic chemical pesticides effluent with proper optimisation.

Keywords: *Synthesis, Nanoceria, mancozeb, wastewater, and photocatalytic degradation.*

1. Introduction

Pesticides are part of the major water pollutants or contaminants throughout the globe. Synthetic pesticides are playing a critical role in food production and global sustainability. These chemicals have a broad range of applications, including controlling weeds and insect infestations in agricultural fields, and managing pests and diseases-carrying organisms like mosquitoes, ticks, rats, and mice in both residential, commercial and public areas (Kim et al., 2016). However, because pesticides do not target a specific species, there are concerns about the potential environmental hazard associated with exposure, through different routes, such as the presence of pesticide residues in water and food (Kim, et al. 2016; Chang 2018; Vijgen et al. 2018). Moreover, studies have revealed that pesticide residues were found to be present in the blood and living system (Bonvoisin et al., 2020; Chang, 2018; El-Alfy et al., 2019; Nicolopoulou-Stamati & , Sotirios Maipas, Chrysanthi Kotampasi, 2016; Walker et al., 2022; Zhao et al., 2020).

Mancozeb MCZ pesticide is one of the most widely used fungicides to protect fruits, crops and vegetables (Bao et al., 2022). The cost and effectiveness of this fungicide made it accessible to farmers all over the world. Studies have shown that mancozeb accounts for about 20% of the global fungicide market (Bao et al., 2022). In terms of its chemical composition, mancozeb is a combination of polymerized complexes of ethylene-bis-dithiocarbamate with both Manganese and Zinc in a 1:1 ratio. When consumed, mancozeb is metabolized in the body and produces a primary urine metabolite called ethylene-bis-thiourea (ETU) in a ratio of approximately 1:2 (Mandić-Rajčević et al., 2020; Quds et al., 2022; Saraiva et al., 2021). Furthermore, mancozeb has been associated with various health hazards due to its continued widespread use among farmers and its chemical nature.

In a research conducted by (Morales-Ovalles et al., 2018), examinations of tissue and cell structures of a particular organism revealed that there was a rise in cell death, inflammation in the nervous system, and loss of the protective coating around nerve cells (demyelination) as a result of the pesticide. These findings indicate that mancozeb caused harmful effects on cells responsible for producing hormones in the hypothalamus through induced cytotoxicity in a male mouse. Analysis of the tissue structure of mice exposed to MCZ by (Bao et al., 2022) indicated that there was harm done to the structure of their ovaries and that there was an increase in the process of cell death known as apoptosis. These findings suggest that MCZ can

Authors information:
[a]Department of Environmental Science, GITAM School of Science, GITAM (Deemed to be University), Visakhapatnam, A.P. INDIA. Email: mahdi.d@fur.edu.ng[1]; vabbaraj@gitam.edu[2]
[b]Department of Chemistry, GITAM School of Science, GITAM (Deemed to be University), Visakhapatnam, A.P. INDIA. Email: vnutulap@gitam.edu[3]
[c]Department of Environmental Science, Federal University Dutse, Jigawa State, NIGERIA. Email: mahdi.d@fur.edu.ng[1]
*Corresponding Author: mahdi.d@fur.edu.ng

Received: July 26, 2023
Accepted: November 29, 2023
Published: December 31, 2024

DOI: https//doi.org/10.22452/mjs.vol43no4.3
Malaysian Journal of Science 43(4): 20-30 (December 2024)

interfere with the normal functioning of the mitochondrial respiratory chain, leading to a decoupling of oxidative phosphorylation and the production of oxidative stress, ultimately resulting in injury to the ovaries and cell death in mice

As such, it is crucial to come up with means to deter this menace of water pollution by pesticides. Researchers and scientists took several measures throughout the globe to come up with suitable alternatives to pesticides, suitable, effective and cheap clean-up or treatment methods and awareness. Several conventional measures for wastewater treatment that include; physical and chemical methods have been in use with issues at one point or another. The realization and validation of particle size as one of the major factors that influence the physicochemical properties of a material (Keerthana et al. 2022; Singh et al. 2022), nanomaterials have recently gotten more attention from researchers and industries to harness their capabilities in today's world.

A semiconductor cerium oxide is getting the attention of scientists and researchers due to its unique nature, properties and abundance. Cerium oxide CeO_2 nanoparticles are becoming significant in our societies and are in use at different levels of civilization. Studies have shown that CeO_2 nanoparticles (NPs) have gained significant consideration from researchers in recent times due to their distinctive structure and attractive properties, making them a highly promising material for a variety of applications (Muduli and Ranjan 2022; Muthuvel et al. 2020). It possesses distinctive chemical and thermal stability, high conductivity, reliable oxygen storage capacity, the ability to absorb UV light, catalytic activity and a broad energy band gap of around 3.19 eV (Eka Putri et al., 2021). These nanoparticles can be utilized in various industrial products such as photocatalysts, sunscreens, polishing agents, and sensor applications, among others (Muduli and Ranjan 2022; Pradeepa and Nayaka 2022; Muthuvel et al. 2020).

Cerium oxide (CeO2) is a type of semiconductor material that exhibits n-type conductivity. This material possesses unique characteristics, such as the ability to catalyze both metal oxidation and reduction reactions through electronic transitions between Ce^{3+} and Ce^{4+} (Kumaraguru et al., 2022). It also has high ionic mobility and the capability to store and release oxygen (Kumaraguru et al. 2022; Shetty et al. 2022; Muduli and Ranjan 2022). Studies involving applications of cerium oxide nanoparticles are reported in recent literature which include; (Lin et al., 2021) for anti-oxidative and anti-reduction regarding ROS, (Mohamed, 2021) involving acute oral administration of the particle for suppressing lead acetate genotoxicity, (Samai & Bhattacharya, 2018) enhanced photocatalytic activity in wastewater treatment for dye degradation, (Pradeepa & Nayaka, 2022) electrochemical investigation of pantoprazole, (Eka Putri et al., 2021) high anti-microbial activity, (Muthuvel et al., 2020) photocatalytic degradation of methyl orange dye and anti-microbial activity, (Miri et al., 2021) for photocatalytic degradation of organic pollutants and (Kashyap et al., 2022) for effective removal of uranium from aqueous solution.

Nanoceria or cerium oxide nanoparticle is a great sorbent or catalyst for the degradation and destruction of persistent environmental pollutants. Despite its wide range of applications, the particles' utilisation for different chemical pesticides in wastewater is still lagging. More focus is given to its photocatalytic activity in the degradation of dye and organophosphate pesticides, especially parathion. As such, in this study, we aim to explore the intrinsic capacity of nanoceria synthesized via the coprecipitation method for the degradation of a carbamate pesticide Mancozeb.

2. Materials and Methods

Chemicals

The chemicals used were of analytical reagent grade and were used with no further purification. Cerium nitrate hexahydrate ($Ce(NO_3)_3.\ 6H_2O$), Potassium carbonate (K_2CO_3), acetonitrile HPLC grade and ethanol were all purchased from Merk company (India), Mumbai. Dithiocarbamate pesticide/Mancozeb 75 % wp was obtained from the farmer's market in Visakhapatnam, Andhra Pradesh state of India. Millipore water/Deionized water was used throughout the experiments.

Synthesis of Cerium Oxide NPs

Cerium oxide NPs were synthesized using a simple coprecipitation method as adopted from the work of (Farahmandjou et al., 2016) and reported in our previous work (Sani et al., 2023). Specifically, two separate solutions of 0.02 M cerium III nitrate and 0.03 M potassium carbonate were carefully prepared by dissolving 2.17 g and 1.036 g respectively in 2 separate 250 ml volumetric flasks. 50 ml of cerium III nitrate was weighed in a conical flask and placed under a burette containing 20 ml of potassium carbonate on a magnetic stirrer. Drops of potassium carbonate were added into the conical flask on the magnetic stirrer through the wall of the container with constant stirring. The pH of the system was maintained at 6 by adding millipore water into the solution. After constant stirring for 3 hours, a white precipitate of cerium III carbonate was formed which was further dried in a hot air oven at 65 ^oC for 2 hours. The particles were later dried to room temperature and aged at 220 ^oC for 2.5 hours which gives brownish particles of nanoceria. The particles were later calcinated at 600 ^oC in a muffle furnace for 3 hours to obtain the pure cerium oxide nanoparticles.

The whole procedure was repeated multiple times until the required quantity of the nanoparticles were obtained for further analysis.

Characterization

The structural characterization processes were conducted to ascertain the formation of cerium oxide nanoparticles through the above-mentioned method. Scanning Electron Microscopy SEM was employed for surface analysis/morphology analysis using SEM-EDAX Jeol 6390 LA/OXFORD XMXN with accelerating voltage of 0.5 to 30 kv, magnification of 300,000 times and tungsten filament. Elemental analysis was conducted by Energy Dispersive X-Ray Spectroscopy EDAX using the same facility with

DOI: https//doi.org/10.22452/mjs.vol43no4.3
Malaysian Journal of Science 43(4): 20-30 (December 2024)

an EDAX resolution of 136 eV and detector area of 30 mm^2.

The particles' crystal structure and crystallite size were determined by powder X-Ray Diffraction PXRD Brucker D8 advance. The scan type and mode are coupled two theta/theta and continuous scan respectively. The scanning begins at 10.000° and ends at 79. 994° at an interval of 0.020° and a temperature of 25 °C/room temperature. Fourier transform Infrared spectroscopy was employed for spectral analysis of the functional groups present. It was achieved using FTIR spectrophotometer Nicolet iS5O with IR source, DTGS KBr detector and KBr beam splitter. A total number of 32 sample scans were conducted at the collection length of 47.3 seconds with a resolution of 4.000. The FTIR range for the analysis was 500-4000 cm^{-1} wavenumber.

Preparation of Different Concentrations of Pesticides

Three standard concentrations of the mancozeb 75% wp were prepared by dissolving certain weights of the powder mancozeb in millipore water to produce 3 different concentrations of 100 ppm, 50 ppm and 10 ppm. The standards were prepared by dissolving 25 mg, 12.5 mg and 2.5 mg of the 75% wp mancozeb for 100 ppm, 50 ppm and 10 ppm respectively into 250 ml volumetric flasks. Each prepared pesticide solution was immediately used for sample preparation and control.

2.5 Degradation Experiments

The photocatalytic degradation and removal of mancozeb pesticide from wastewater was carefully conducted from 13th December 2022 to 10th March 2023 at GITAM University, Visakhapatnam, Andhra Pradesh, India. For each batch of the experiment, temperature, UV index, Humidity and atmospheric pressure were noted and recorded to understand the suitable atmospheric conditions for better degradation.

100 ml of each of the concentrations of the pesticides were exposed to 2 quantities of nanoceria 50 mg and 10 mg which were carefully mixed using a magnetic stirrer under dark conditions and a control setup with no nanoceria. Before exposure to natural solar irradiation, the samples were kept in the dark for 30 minutes to achieve adsorption-desorption equilibrium. Table 1 below shows the different compositions of the samples.

Table 1. Sample composition

Sample name	Pesticide initial concentration (ppm)	Quantity of nanoparticle Cerium oxide NPs (mg)
MCE-1	100	50
MCE-2	100	10
MCE-3	50	50
MCE-4	50	10
MCE-5	10	50
MCE-6	10	10

After exposure to natural solar irradiation, a certain amount of the sample was withdrawn after every 30 minutes from each of the samples which were wrapped in foil paper to avoid light penetration for further analysis. Subsequently, the samples were collected/withdrawn for six consecutive rounds until 3 hours (0.5 hour, 1 hour, 1.5 hours, 2 hours, 2.5 hours and 3 hours), wrapped in foil paper and kept in the dark after recording the pH at each point. Furthermore, all the samples were centrifuged at 3500 rpm for 10 minutes and the supernatant liquids were separately collected for further analysis. The settled nanoparticles were collected and washed thrice with millipore water and ethanol and used for other rounds of the degradation experiment. The same procedure was applied for the control with no photocatalyst.

Shimadzu 1800 UV spectrophotometer was used to determine the absorbance and concentration of each of the samples and control. The absorbance was recorded at the range of 200-400 nm wavelength whereas the initial and final concentrations of the pesticide were determined at λ_{max} wavelength of 240 nm. For each round of the concentration determination, a set of standards were carefully prepared using the serial dilution method to form a linear graph of the concentration and absorbance.

Moreover, three optimization parameters considered for this research were; the initial concentration of the pesticide, the amount of the photocatalyst/nanoparticle, and irradiation time. However, the calcination temperature of the nanoceria and environmental conditions of each experimental period were considered. Moreover, the environmental/atmospheric conditions were not controlled but only recorded, and additional runs of the experiment were conducted whenever there was a reasonable change in the temperature and UV index (three scales of UV index; 7 as high, 8, 9, and 10 as very high and 11, 12 as extreme). The reason for these choices is for feasibility in field application and other parameters may be difficult to control in the field.

The degradation efficiency was determined using the following formula;

$$\% \text{ degradation/degradation efficiency} = \frac{Co-Cf}{Co} \times 100 \quad (1)$$

Where Co is the initial concentration of mancozeb pesticide and Cf is the final concentration of mancozeb pesticide.

DOI: https//doi.org/10.22452/mjs.vol43no4.3
Malaysian Journal of Science 43(4): 20-30 (December 2024)

3. Results and Discussion

Synthesized nanoceria

Cerium oxide nanoparticles were successfully synthesized using the above-mentioned method and the result of the synthesis is presented below.

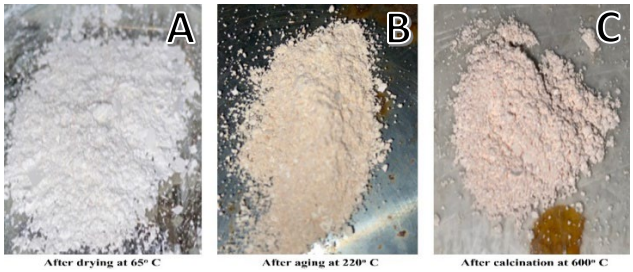

Figure 1. Synthesized nanoparticles at various points of synthesis

Figure 1 captioned A, B, and C shows the different stages of the nanoceria synthesis with A showing the drying of the cerium carbonate at 65 °C to B showing the ageing of the product at 220°C and C revealing the calcination at 600 °C to form the cerium oxide nanoparticles. The physical nature and colour of the synthesized NPs are in agreement with the findings of (Miri et al., 2020) where a brownish-yellow powder particle is formed.

Characterization

Scanning Electron Microscopy SEM

Scanning electron microscopy SEM which is a morphology analysis method was employed for the determination of the surface morphology of the NPs.

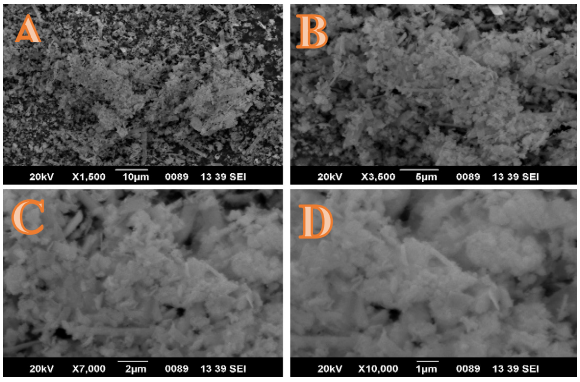

Figure 2. Scanning electron microscopy showing the morphology of the particles

From the images obtained from SEM Fig. 2, it can be observed that there exists some agglomeration at various points which may be due to various factors including temperature and solvents employed for washing the NPs. As revealed in C and D images with 1 and 2 µm resolution images, the morphology of the particles is somehow spherical with clusters of thin plate shapes of irregular sizes which may be a result of the agglomeration and annihilation process. Similar findings for the spherical surface morphology was reported by (Farahmandjou et al., 2016) and the thin plate shapes of irregular sizes were revealed by the work of (Janos et al., 2014).

Energy Dispersive X-Ray Spectroscopy EDAX

The elemental composition of the synthesized NPs was determined by the SEM-EDAX facility where the peaks for cerium and oxygen are obtained on the spectrum.

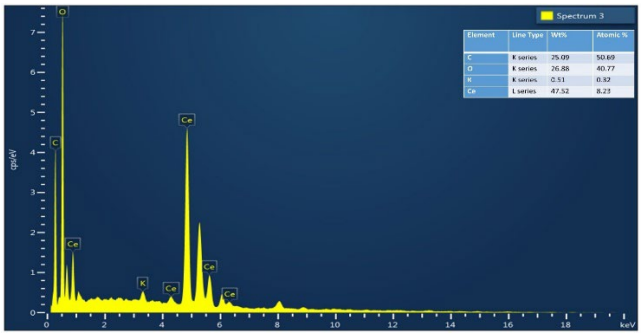

Figure 3. EDAX spectrum showing the elemental composition of the particles

The EDAX spectrum in Fig. 3 above revealed the elemental composition of the NPs with peaks for cerium, oxygen, carbon and potassium which confirms the existence of the elements in the synthesized NPs. The weight of cerium was found to be 47.52 % and that of oxygen found to be 26.88 %

3.2.3 Powder X-Ray Diffraction PXRD

The crystal structure, phase and crystal size of the synthesized nanoceria were determined by PXRD analysis which involves analyzing the diffraction pattern of scattered X-rays by the planes of CeO_2 NPs.

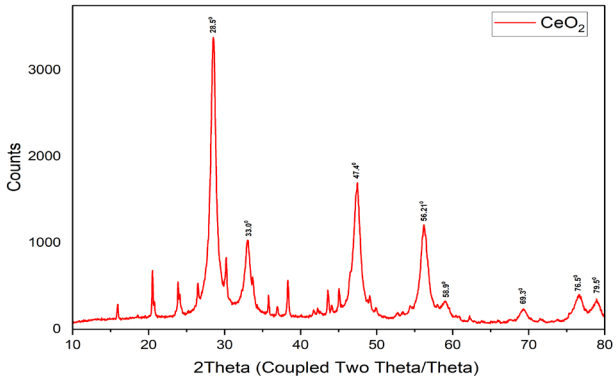

Figure 4. PXRD spectrum showing the crystallography and particle size under the diffraction peaks

Figure 4 presents the XRD peaks of the annealed/calcinated NPs at various points. The peaks exhibited at 28.507 °, 33.032 °, 47.446 °, 56.214 °, 58. 994 °, 69.327 °, 76.598 ° and 79.54 ° correspond to (111), (200), (220), (311), (222), (400), (311) and (420) planes of cubic fluorite structure of nanoceria. The planes and diffracted angles are in agreement with the results of JCPDS (Farahmandjou et al., 2016; Janoš et al., 2022; Keerthana et al., 2022).

DOI: https//doi.org/10.22452/mjs.vol43no4.3
Malaysian Journal of Science 43(4): 20-30 (December 2024)

The crystallite size was computed from the XRD data using the Debye- Scherrer equation,

$$d = \frac{0.9\,\lambda}{\beta\cos\theta} \quad (2)$$

where; d is the crystallite size

λ is the wavelength of Cu Kα radiation

β is the full-width at half maximum (FWHM) of the diffraction peak

Θ is the diffraction angle

The crystallite size of the synthesized particle was found to be 27nm.

Fourier Transform Infrared Spectroscopy FTIR

Fourier transform Infrared spectroscopy FTIR was employed for the identification of the functional groups present which involves the detection of vibration bands of organic and inorganic species.

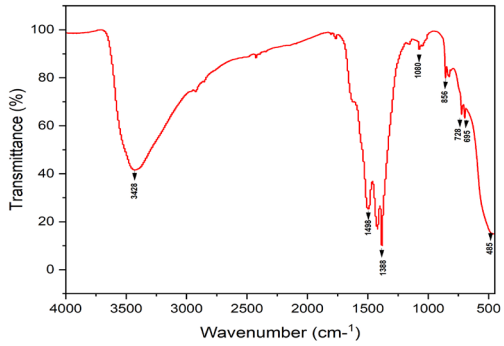

Figure 5. FTIR spectrum showing the functional groups present

The peaks as presented in Fig. 5 spectrum revealed the functional groups present in the sample, reagents and solvents used for the synthesis. The broad peak at 3428.19 cm^{-1} may be attributed to the –OH stretching of water molecules used as a solvent for the synthesis process. The H-O-H bending vibration of water molecules may be responsible for the transmittance band at 1498.06 cm^{-1} which is somewhat similar to the band reported by (Raees et al., 2022). However, the transmittance band below 500 cm^{-1} wavenumbers may be a result of the stretching vibration band of Ce-O (Janoš et al., 2022; Raees et al., 2022). However, in other studies, the vibration band of Ce-O was reported to be at exactly 500 cm^{-1} wavenumber (Farahmandjou et al., 2016).

Photocatalytic Degradation of Mancozeb

This experiment was conducted in batches under natural environmental conditions. For each sample setup, 3 different concentrations of the mancozeb pesticide were exposed to 2 quantities of the photocatalyst.

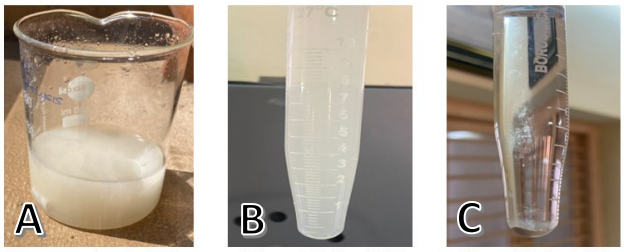

Figure 6. Photocatalytic degradation process

Figure 6 A, B, and C above shows some of the stages of the degradation experiment ranging from A, exposure of the sample and control to natural solar irradiation to B, collection/withdrawal of 10 ml of the sample at the 30-minute interval for centrifuging and C showing sample and settled nanocatalyst after centrifugation.

Uv Absorbance of The Samples at Different Time Intervals

All the samples have shown a great decrease in absorbance over time with little variation between 2-3 hours. By Beer's law which relates the concentration of a particular solution with light absorbance, the initial and final mancozeb residue and the reaction kinetics were determined.

DOI: https//doi.org/10.22452/mjs.vol43no4.3
Malaysian Journal of Science 43(4): 20-30 (December 2024)

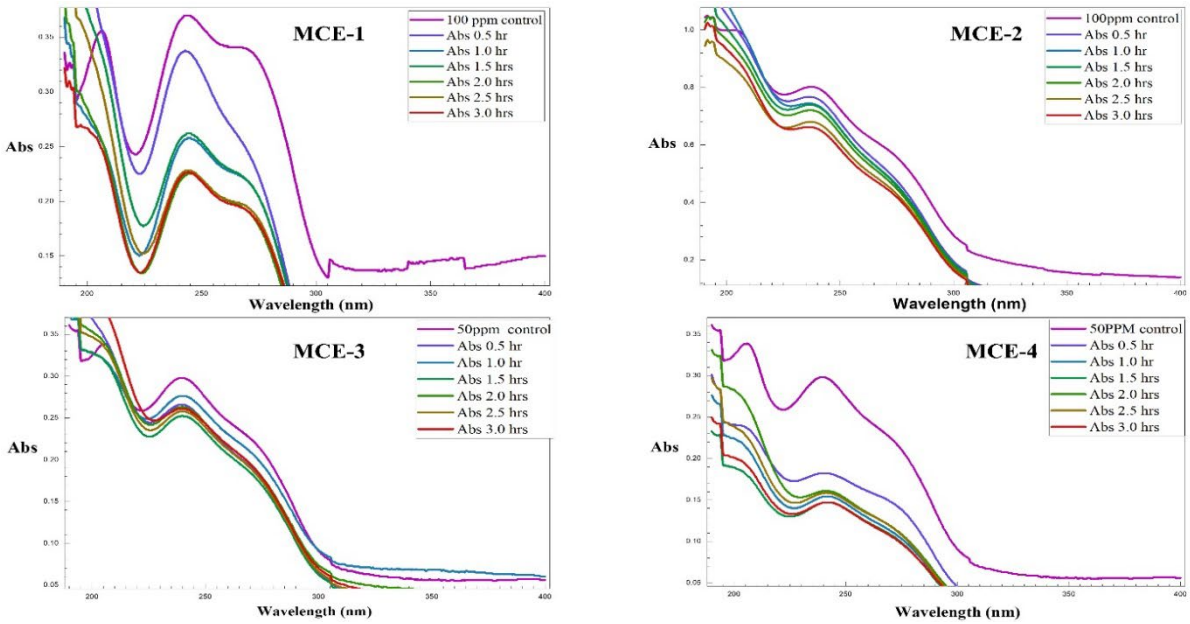

Figure 7. UV Absorbance spectrum for MCE-1, MCE-2, MCE-3 and MCE-4

From Figure 7, it can be observed that MCE-1 shows a sharp change in the absorbance of the solution which can be considered a strong indication of a decrease in the concentration of the pesticide. From the spectrum, it can also be observed that the control setup with no photocatalyst has the highest absorbance. Although, after 2 hours of the experiment, there was not much change in the UV absorbance with a few rounds showing a slight increase in the absorbance over time.

A similar scenario as MCE-1 above was observed in MCE-3 with a slight increase in absorbance at 2.5 and 3.0 hours. Although, the decrease in the absorbance for MCE-3 is quite lower when compared with MCE-1. A similar amount of the catalyst was used for the samples.

However, MCE-4 with 10 mg photocatalyst has shown the best decrease in absorbance after several runs under natural environmental conditions. In this sample setup, there was a slight difference between 2 and 3 hours with 2.5 hours having greater absorbance as compared to the former. In general, there was a great decrease in the absorbance regarding this setup after several runs. Moreover, a lower amount of the NPs has shown greater action against the pesticide residue in comparison with the standard which may be attributed to the high light penetration.

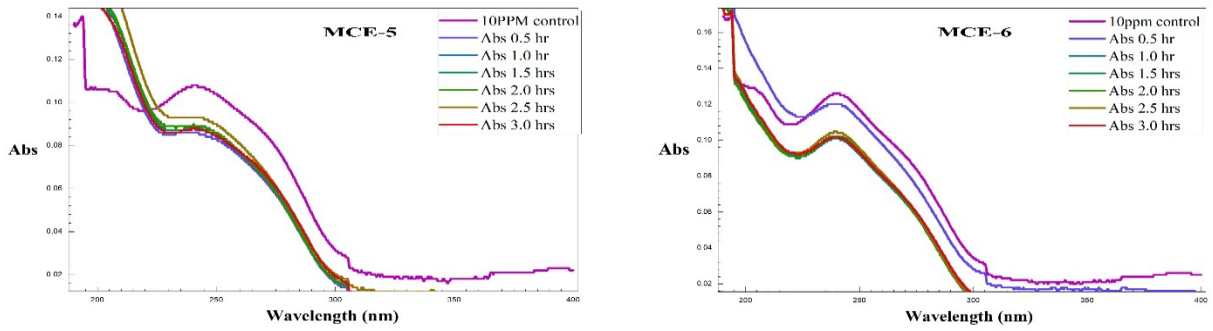

Figure 8. UV Absorbance spectrum for MCE-5 and MCE-6

Decreasing the concentration of mancozeb to 10 ppm shows yet another decrease in the absorbance with a similar pattern as compared to the setups with 50 mg photocatalyst as shown in Fig. 8. A similar scenario that happens to all the samples with 10 mg photocatalyst occurs in MCE-6. The absorbance pattern at 2.0, 2.5 and 3.0 hours of exposure to natural solar irradiation and 10 mg photocatalyst shows a close absorbance peak. This can be considered as an indication that the photocatalysis process may have reached a saturation level at between 2-3 hours of irradiation time.

Determination of the Concentrations and Degradation Efficiency

The concentrations at time t of the MCZ residue were determined at a maximum wavelength absorbance of 240 nm ƛmax using Shimadzu UV spectroscopy which was computed from the UV absorbance spectrum.

DOI: https//doi.org/10.22452/mjs.vol43no4.3
Malaysian Journal of Science 43(4): 20-30 (December 2024)

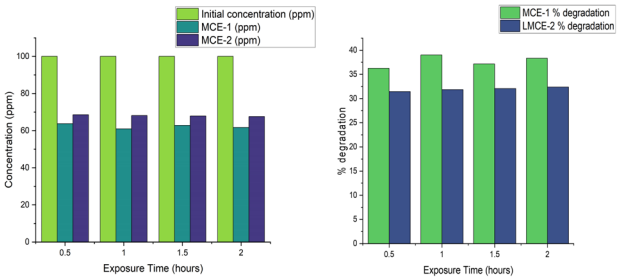

Figure 9. Initial and final concentration and percentage degradation of MCE-1 and MCE-2 over time

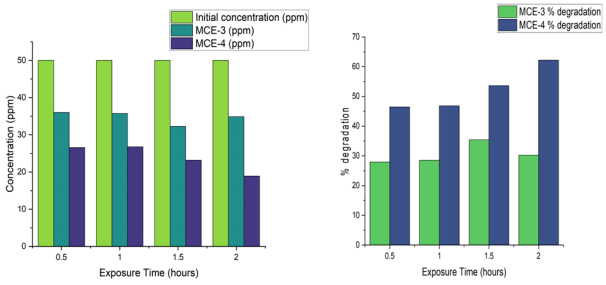

Figure 10. Initial and final concentration and percentage degradation of MCE-3 and MCE-4 over time

Concerning the first 2 sample setups; MCE-1 and MCE-2 containing 100 ppm mancozeb pesticide and 2 quantities of 50 mg and 10 mg NPs respectively, the initial and final concentrations were determined including that of control at different time intervals. From Fig. 9, it was observed that the initial concentration of each of the samples continued to decrease with an increase in the irradiation time. However, after 2 hours of exposure, no significant change was observed for the samples signifying that the process may have slowed down. For MCE-1, the initial concentration decreased by 36% at 0.5 hours exposure time to about 39.0% after an hour and stabilized at 38.3% degradation at 2 hours and above. However, there was a lower degradation or percentage degradation in regards to MCE-2 with 10 mg NPs quantity where only 31.5% degradation was observed at 0.5 hour irradiation time with a gradual increase in the degradation to about 32.4%. A similar scenario occurs here where the decrease in the concentration was slow after 2 hours. The activation of the photocatalytic reaction or process begins only when the surface of the photocatalyst is exposed to illumination. Consequently, the reaction zone, which corresponds to the top layer of the solution experiencing the highest intensity, becomes the most active area for pollutant degradation. However, when the initial pesticide concentration is high, it tends to excessively adhere to the surface of nanocatalysts thereby obstructing the necessary light energy penetration on the surface (Sraw et al., 2022). Moreover, the initial degradation efficiency was revealed to show a faster rate which subsequently stabilized with time and resulted in a small change in the concentration after 0.5 hour of irradiation.

Generally, for MCE-1 and MCE-2 samples setup, the percentage degradation was higher in the former which may be attributed to many factors including the quantity of the photocatalyst. When compared at each time interval, MCE-1 with 50 mg NPs was found to possess higher catalytic action than MCE-2 with 10 mg NPs. As can be observed in the figure, a 50 mg nanocatalyst was found to be more efficient towards the degradation of 100 ppm MCZ than a 10 mg nanocatalyst with the same MCZ concentration.

However, MCE-3 and MCE-4 samples setup were found to exhibit an entirely different pattern from MCE-1 and MCE-2. From Fig. 10, it can be observed that the initial 50 ppm concentration of the pesticide has shown more degradation in MCE-4 with 10 mg NPs than in MCE-3 with 50 mg NPs. However, a similar pattern regarding exposure time applies to all. At 0.5 hour exposure time, only 27.9% was degraded which was further increased to about 35% at 1.5 hours and stabilized at 30.3% at 3 hours and above. It is crucial to note the broad difference in the degradation between MCE-3 and MCE-4. About 46.5% degradation occurs at 0.5 hour exposure which is greater than the 2 hours and above for MCE-3. Additionally, the degradation continues like this for all the experiments with regards to MCE-4 with a mean percentage degradation of about 62.2% at 2 hours exposure time.

MCE-4 with 10 mg NPs was found to possess a higher degradation capacity than the 50 mg in MCE-3. Therefore, the higher quantity of the NPs/photocatalyst may not be crucial at this concentration of 50 ppm mancozeb. It may also be inferred that lower concentrations like 50 ppm of this setup as compared to 100 ppm of the previous setup may have given more room for catalytic degradation.

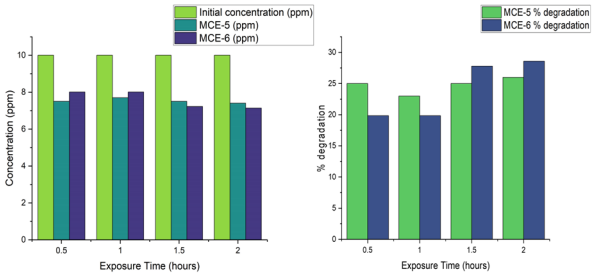

Figure 11. Initial and final concentration and percentage degradation of MCE-5 and MCE-6 over time

MCE-5 and MCE-6 sample setups follow similar patterns to MCE-3 and MCE-4. Although the degradation was found to be low after several runs as compared to the setup of the previous sample. The degradation pattern obtained may be used to infer that lower concentrations of MCZ do not require a higher quantity of the NPs/photocatalysts. Although, at 0.5 and 1-hour exposure, the degradation efficiency was higher for MCE-5 than MCE-6, after 1 hour the efficiency of the MCE-6 was higher with about 28.6%

DOI: https//doi.org/10.22452/mjs.vol43no4.3
Malaysian Journal of Science 43(4): 20-30 (December 2024)

degradation as can be observed in Fig 11.

The above table shows the percentage degradation between the 2 samples at various time intervals. MCE-6 with 10 ppm mancozeb pesticide and 10 mg NPs/photocatalyst was found to possess a lower initial degradation capacity as compared to MCE-5. However, from 1.5 hours, the degradation efficiency was higher for MCE-6 than that MCE-5.

Optimization

(Ederer et al., 2019) revealed that pesticides like other organic pollutants can degrade on the surface of the nanoceria with a reaction mechanism similar to a hydrolysis reaction happening in the solvent/water. Additionally, (Janoš et al., 2022) reported that hydroxyls play an important role in the degradation of organophosphate pesticides in the presence of nanoceria. Therefore, the solvent involved in these processes also plays a crucial role in the activity. Nanoceria was revealed to be a reactive sorbent in the destruction of parathion methyl together with other organophosphate but, the process was found to be greatly affected by the solvent involved (Janos et al., 2014). In this study, our focus was on the field application of the particle where wastewater will be the solvent during the degradation process.

Throughout the experiment, MCE-1 and MCE-2 were exposed to the same experimental condition with only the quantity of the NPs different. The same applied to MCE-3 and MCE-4, and MCE-5 and MCE-6. The initial and final concentrations of the pesticide were determined at each level of the experiment after considering all the stated conditions. From the findings of this research, it was observed that the initial concentration of the pesticide, the exposure/irradiation time, the quantity of the nanoparticles/photocatalyst, calcination temperature, and atmospheric conditions that include temperature and UV index UVI play a significant role in the degradation process. Each of the aforementioned conditions was tested during the study.

There was a little change in the absorbance in the dark before exposure to natural solar irradiation, possibly due to adsorptions and desorption equilibrium. Also, the reuse of the NPs was tested after 3 rounds with little change in its activity. The light sensitivity of nanoceria was also tested during the experiment when comparing the dark reaction before exposure to solar irradiation and the light reaction after exposure. The photocatalytic activity of nanoceria was reported by multiple researchers (Janoš et al. 2022; Keerthana et al. 2022; El Desouky, Saadeldin, and El Zawawi 2022; Samai and Bhattacharya 2018; Muthuvel et al. 2020)

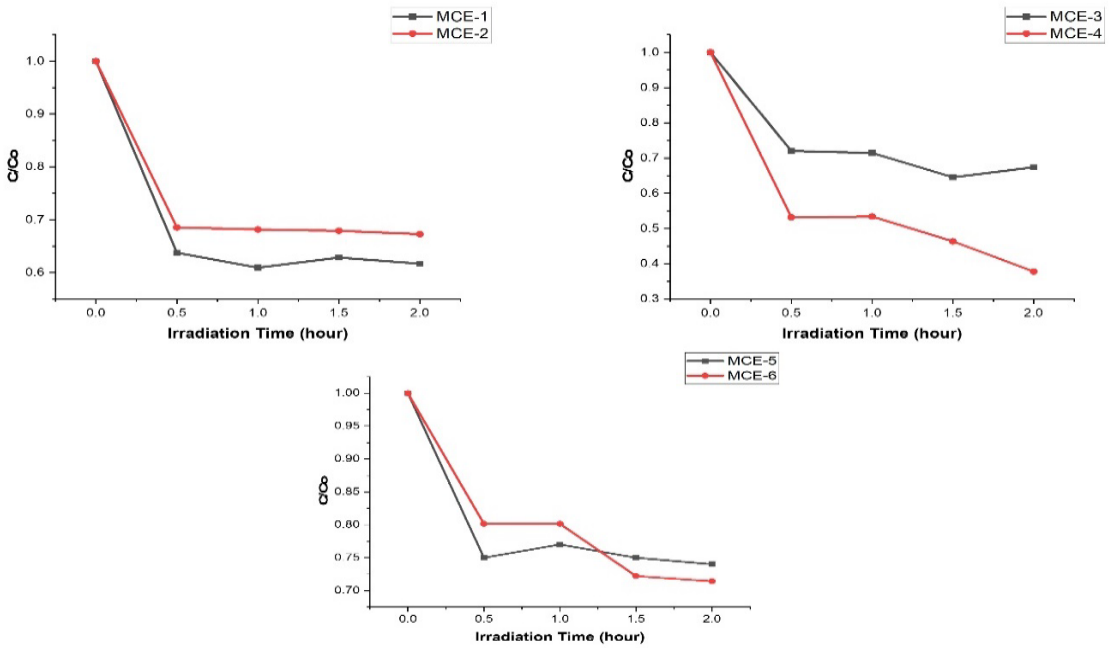

Figure 12. Photocatalytic degradation rate for 3 different concentrations of 100 ppm, 50 ppm and 10 ppm with 50 mg and 10 mg of the photocatalyst

Figure 12 revealed the degradation rate of the samples with all the setups showing very fast initial degradation activity followed by a subsequent slower activity to stabilization at a certain point. As shown in the degradation figures, the initial concentration of the pesticide may be said to affect the degradation process with 100 ppm concentration showing more affinity to degradation with 50 mg NPs while lower concentrations of 50 ppm and 10 ppm show a different trend with 10 mg NPs giving best results. As such, it may be inferred that with increasing the quantity of the NPs, only higher concentrations like 100ppm mancozeb show more degradation which may be due to adsorption as a result of more NPs with more surface area-to-volume ratio and/or photocatalysis due to high concentration of the pesticide. However, lower concentrations like 50 ppm and 10 ppm show a different trend with more degradation with 10 mg NPs. This may be a result of many factors including more room for light penetration and photocatalysis that involves the split of holes and electrons between the valance and conduction band which attacks the pesticide from different angles in the reaction.

Throughout the experiment, the exposure time was found to be

DOI: https//doi.org/10.22452/mjs.vol43no4.3
Malaysian Journal of Science 43(4): 20-30 (December 2024)

an important factor where the more the exposure time the higher the degradation until 2 hours after which the process stabilized with few exceptions. Other studies with nanoceria have also revealed similar results regarding irradiation time (Keerthana et al. 2022; Samai and Bhattacharya 2018; Miri et al. 2021; Janos et al. 2014; Keerthana et al. 2021; Janoš et al. 2022). The calcination temperature was tested between the aged and calcinated products. It was observed that the calcinated product at 600 ^{o}C was found to be more active than the others which is in agreement with the findings of (Ederer et al., 2019; Janos et al., 2014) with calcination or annealed temperature of between 500 ^{o}C and 700 ^{o}C. For the atmospheric conditions, temperature and UV index considered were found to play an important role in the entire process. This was determined during the period of the experimentation. In the experiments conducted during the month of December when the temperature was moderate 26-28 ^{o}C in Visakhapatnam, Andhra Pradesh with a moderate to high UV index of 5-7, the rate of degradation was found to be low as compared to experiments in the month of February-march with a temperature of about 29-32 ^{o}C and very high UV index 8-10. As such, the degradation efficiency was higher with high UVI which may be a result of the UV portion light's capability to initiate the process of photocatalysis using semiconductor nanoparticles.

Overall, at optimal conditions considered for this research, 50 ppm mancozeb concentration, 10mg quantity of the nanoceria, 2 hours and a very high UV index of 8 to above, nanoceria was able to degrade about 62% of the pesticide under natural solar irradiation. However, with appropriate optimization and doping to reduce the band gap energy of the photocatalyst and improve light absorbance, more degradation may be achieved in a speculated time. The findings of this research are compatible with the photocatalysis of mancozeb nanoformulation using titanium oxide nanoparticles under natural solar irradiation reported by (Daqa et al., 2022). The sharp initial degradation rate followed by subsequent slow degradation rate over time was also reported.

4. Conclusion

The abundance of cerium as compared to other rare earth elements REE and lanthanides and the adsorptive reactivity of cerium oxide has made nanoceria to be significant particles for the destruction of contaminants like pesticides in wastewater and agricultural runoff. Nanoceria was successfully synthesized by a simple coprecipitation method which was further confirmed and ascertained by characterization through SEM, EDAX, XRD and FTIR. The XRD pattern has shown the crystallite shape and size of the synthesized to be cubic structure and 27 nm respectively. Although the SEM images were observed to contain agglomeration at various points, the clusters of thin plate shapes of the NPs were observed on the images. The FTIR analysis revealed a peak at around 500 cm^{-1} wavenumber for cerium oxide functional with other peaks depicting the –OH group in the water molecule and other solvents. EDAX spectra of the synthesized nanoceria have revealed the elemental composition of the particles with high purity. The photocatalytic degradation of the mancozeb pesticide was conducted using the synthesized nanoceria as a photocatalyst which was found to show great activity and efficiency towards the degradation of the mancozeb pesticide. It was observed that the degradation activity of nanoceria was affected by the initial concentration of the pesticide, quantity of photocatalyst, time, calcination temperature and UV index. Nanoceria usually acts as an active sorbent in the destruction of pesticides in wastewater. At optimal conditions considered during this study, nanoceria was found to degrade more than 62% of the initial concentration of the pesticide in 2 hours. Although, only the intrinsic capacity of the particle/nanoceria to act as a photocatalyst was considered with no doping or hole scavenger, the photocatalytic activity of the particle towards mancozeb pesticide is quite significant.

Moreover, it is crucial to note that further studies need to focus more on optimizing the conditions necessary for the photocatalytic activity of nanoceria which include but are not limited to, anneal/calcination temperature, the intensity of UV or source of energy, initial concentration of the contaminant, and nature and amount of dopant for better photocatalysis.

5. Acknowledgement

The authors acknowledge GITAM University, STIC Coaching Institute and Federal University Dutse. Also, the authors are thankful to the anonymous reviewers for their incredible work. Appreciation is extended to the DST analytical chemistry laboratory at GITAM University.

6. Declaration

The authors declare no known competing interests including financial and personal interests.

7. References

Bao, J., Zhang, Y., Wen, R., Zhang, L., & Wang, X. (2022). Low level of mancozeb exposure affects ovary in mice. *Ecotoxicology and Environmental Safety*, *239*, 113670. https://doi.org/10.1016/J.ECOENV.2022.113670

Bonvoisin, T., Utyasheva, L., Knipe, D., Gunnell, D., & Eddleston, M. (2020). *Suicide by pesticide poisoning in India : a review of pesticide regulations and their impact on suicide trends*. 1–16.

Chang, G. R. (2018). Persistent organochlorine pesticides in aquatic environments and fishes in Taiwan and their risk assessment. *Environmental Science and Pollution Research*, *25*(8), 7699–7708. https://doi.org/10.1007/S11356-017-1110-Z/TABLES/3

Daqa, W. M., Alshoaibi, A., Ahmed, F., & Rao, T. N. (2022). Synthesis and Characterization of Nanoformulation of the Broad-Spectrum Enzyme Inhibitor Mancozeb by Polyethylene Glycol Capping and Its Dissipation Kinetics in Water Using TiO2 Nanoparticles. *Processes*, *10*(12). https://doi.org/10.3390/pr10122733

Ederer, J., Sˇtastn, M., DošekDošek, M., Henych ab, J., &

DOI: https//doi.org/10.22452/mjs.vol43no4.3
Malaysian Journal of Science 43(4): 20-30 (December 2024)

JanošJanoš, P. (2019). *Mesoporous cerium oxide for fast degradation of aryl organophosphate flame retardant triphenyl phosphate*. https://doi.org/10.1039/c9ra06575j

Eka Putri, G., Rilda, Y., Syukri, S., Labanni, A., & Arief, S. (2021). Highly antimicrobial activity of cerium oxide nanoparticles synthesized using Moringa oleifera leaf extract by a rapid green precipitation method. *Journal of Materials Research and Technology*, *15*, 2355–2364. https://doi.org/10.1016/J.JMRT.2021.09.075

El-Alfy, M. A., Hasballah, A. F., Abd El-Hamid, H. T., & El-Zeiny, A. M. (2019). Toxicity assessment of heavy metals and organochlorine pesticides in freshwater and marine environments, Rosetta area, Egypt using multiple approaches. *Sustainable Environment Research*, *29*(1), 1–12. https://doi.org/10.1186/S42834-019-0020-9/TABLES/6

El Desouky, F. G., Saadeldin, M. M., & El Zawawi, I. K. (2022). Synthesis and tuning the structure, morphological, optical, and photoluminescence properties of heterostructure cerium oxide and tin oxide nanocomposites. *Journal of Luminescence*, *241*, 118450. https://doi.org/10.1016/J.JLUMIN.2021.118450

Farahmandjou, M., Farahmandjou, M., Zarinkamar, M., & Firoozabadi, T. P. (2016). Synthesis of Cerium Oxide (CeO2) nanoparticles using simple CO-precipitation method Article in Revista Mexicana de Fisica · Synthesis of Cerium Oxide (CeO 2) nanoparticles using simple CO-precipitation method. *Revista Mexicana de Física*, *62*(October), 496–499. https://www.researchgate.net/publication/308742876

Janoš, P., Ederer, J., Šťastný, M., Tolasz, J., & Henych, J. (2022). Degradation of parathion methyl by reactive sorption on the cerium oxide surface: The effect of solvent on the degradation efficiency. *Arabian Journal of Chemistry*, *15*(6). https://doi.org/10.1016/j.arabjc.2022.103852

Janos, P., Kuran, P., Kormunda, M., Stengl, V., Grygar, T. M., Dosek, M., Stastny, M., Ederer, J., Pilarova, V., & Vrtoch, L. (2014). Cerium dioxide as a new reactive sorbent for fast degradation of parathion methyl and some other organophosphates. *Journal of Rare Earths*, *32*(4), 360–370. https://doi.org/10.1016/S1002-0721(14)60079-X

Kashyap, K., Khan, F., Verma, D. K., & Agrawal, S. (2022). Effective removal of uranium from aqueous solution by using cerium oxide nanoparticles derived from citrus limon peel extract. *Journal of Radioanalytical and Nuclear Chemistry*, 1–11. https://doi.org/10.1007/S10967-021-08138-4/TABLES/3

Keerthana, M., Malini, T. P., & Sangavi, R. (2021). Efficiency of cerium oxide (CeO2) nano-catalyst in degrading the toxic and persistent 4-nitrophenol in aqueous solution. *Materials Today: Proceedings*, *50*, 375–379. https://doi.org/10.1016/j.matpr.2021.10.082

Keerthana, M., Malini, T. P., & Sangavi, R. (2022). Efficiency of cerium oxide (CeO2) nano-catalyst in degrading the toxic and persistent 4-nitrophenol in aqueous solution. *Materials Today: Proceedings*, *50*, 375–379. https://doi.org/10.1016/J.MATPR.2021.10.082

Kim, K., Kabir, E., & Ara, S. (2016). Science of the Total Environment Exposure to pesticides and the associated human health effects. *Science of the Total Environment*. https://doi.org/10.1016/j.scitotenv.2016.09.009

Kumaraguru, S., Nivetha, R., Gopinath, K., Sundaravadivel, E., Almutairi, B. O., Almutairi, M. H., Mahboob, S., Kavipriya, M. R., Nicoletti, M., & Govindarajan, M. (2022). Synthesis of Cu-MOF/CeO2 nanocomposite and their evaluation of hydrogen production and cytotoxic activity. *Journal of Materials Research and Technology*, *18*, 1732–1745. https://doi.org/10.1016/J.JMRT.2022.03.028

Lin, Y. H., Shen, L. J., Chou, T. H., & Shih, Y. hsin. (2021). Synthesis, Stability, and Cytotoxicity of Novel Cerium Oxide Nanoparticles for Biomedical Applications. *Journal of Cluster Science*, *32*(2), 405–413. https://doi.org/10.1007/S10876-020-01798-4/FIGURES/6

Mandić-Rajčević, S., Rubino, F. M., & Colosio, C. (2020). Establishing health-based biological exposure limits for pesticides: A proof of principle study using mancozeb. *Regulatory Toxicology and Pharmacology*, *115*, 104689. https://doi.org/10.1016/J.YRTPH.2020.104689

Miri, A., Beiki, H., Najafidoust, A., Khatami, M., & Sarani, M. (2021). Cerium oxide nanoparticles: green synthesis using Banana peel, cytotoxic effect, UV protection and their photocatalytic activity. *Bioprocess and Biosystems Engineering*, *44*(9), 1891–1899. https://doi.org/10.1007/S00449-021-02569-9/FIGURES/10

Miri, A., Sarani, M., & Khatami, M. (2020). *Nickel-doped cerium oxide nanoparticles: biosynthesis, cytotoxicity and UV protection studies*. https://doi.org/10.1039/c9ra09076b

Mohamed, H. R. H. (2021). Acute Oral Administration of Cerium Oxide Nanoparticles Suppresses Lead Acetate–Induced Genotoxicity, Inflammation, and ROS Generation in Mice Renal and Cardiac Tissues. *Biological Trace Element Research*, *200*(7), 3284–3293. https://doi.org/10.1007/S12011-021-02914-9/FIGURES/7

Morales-Ovalles, Y., Miranda-Contreras, L., Peña-Contreras, Z., Dávila-Vera, D., Balza-Quintero, A., Sánchez-Gil, B., & Mendoza-Briceño, R. V. (2018). Developmental exposure to mancozeb induced neurochemical and morphological alterations in adult

DOI: https//doi.org/10.22452/mjs.vol43no4.3
Malaysian Journal of Science 43(4): 20-30 (December 2024)

male mouse hypothalamus. *Environmental Toxicology and Pharmacology*, *64*, 139–146. https://doi.org/10.1016/J.ETAP.2018.10.004

Muduli, S., & Ranjan Sahoo, T. (2022). Green synthesis of cerium oxide, Co-doped cerium oxide nanoparticles and its dielectric properties. *Materials Today: Proceedings*. https://doi.org/10.1016/J.MATPR.2022.07.308

Muthuvel, A., Jothibas, M., Mohana, V., & Manoharan, C. (2020). Green synthesis of cerium oxide nanoparticles using Calotropis procera flower extract and their photocatalytic degradation and antibacterial activity. *Inorganic Chemistry Communications*, *119*, 108086. https://doi.org/10.1016/J.INOCHE.2020.108086

Nicolopoulou-Stamati, P., & , Sotirios Maipas, Chrysanthi Kotampasi, P. S. and L. H. (2016). *Chemical Pesticides and Human Health : The Urgent Need for a New Concept in Agriculture*. *4*(July), 1–8. https://doi.org/10.3389/fpubh.2016.00148

Pradeepa, E., & Nayaka, Y. A. (2022). Cerium oxide nanoparticles via gel-combustion for electrochemical investigation of pantoprazole in the presence of epinephrine. *Journal of Materials Science: Materials in Electronics*, *33*(23), 18374–18388. https://doi.org/10.1007/S10854-022-08692-X/TABLES/2

Quds, R., Amiruddin Hashmi, M., Iqbal, Z., & Mahmood, R. (2022). Interaction of mancozeb with human hemoglobin: Spectroscopic, molecular docking and molecular dynamic simulation studies. *Spectrochimica Acta Part A: Molecular and Biomolecular Spectroscopy*, *280*, 121503. https://doi.org/10.1016/J.SAA.2022.121503

Raees, A., Jamal, M. A., Ahmad, A., Ahmad, I., Saeed, M., Habila, M. A., AlMasoud, N., & Alomar, T. S. (2022). Synthesis and characterization of Ceria incorporated Nickel oxide nanocomposite for promising degradation of methylene blue via photocatalysis. *International Journal of Environmental Science and Technology*, *19*(7), 6445–6452. https://doi.org/10.1007/S13762-021-03584-9/FIGURES/6

Samai, B., & Bhattacharya, S. C. (2018). Conducting polymer supported cerium oxide nanoparticle: Enhanced photocatalytic activity for waste water treatment. *Materials Chemistry and Physics*, *220*, 171–181. https://doi.org/10.1016/J.MATCHEMPHYS.2018.08.050

Sani, M. D., Abbaraju, V. D. N. K., & Venugopal, N. V. S. (2023). Photocatalytic degradation and removal of type II pyrethroid pesticide (lambda - cyhalothrin) residue from wastewater using nanoceria for agricultural runoff application. *Journal of Applied and Natural Science*, *9411*, 1219–1229.

Saraiva, M. A., de Carvalho, N. R., Martins, I. K., Macedo, G. E., Rodrigues, N. R., de Brum Vieira, P., Prigol, M., Gomes, K. K., Ziech, C. C., Franco, J. L., & Posser, T. (2021). Mancozeb impairs mitochondrial and bioenergetic activity in Drosophila melanogaster. *Heliyon*, *7*(1), e06007. https://doi.org/10.1016/J.HELIYON.2021.E06007

Shetty, A. N., Kaveri, ·, Kiran, ·, Desai, K., Somanathreddy, ·, & Patil, C. (2022). Green Combustion Synthesis of CeO2 Nanostructure Using Aloe vera (L.) Burm f. Leaf Gel and Their Structural, Optical and Antimicrobial Applications. *BioNanoScience 2022*, *1*, 1–9. https://doi.org/10.1007/S12668-022-01001-0

Singh, P., Mohan, B., Madaan, V., Ranga, R., Kumari, P., Kumar, S., Bhankar, V., Kumar, P., & Kumar, K. (2022). Nanomaterials photocatalytic activities for waste water treatment: a review. *Environmental Science and Pollution Research 2022 29:46*, *29*(46), 69294–69326. https://doi.org/10.1007/S11356-022-22550-7

Sraw, A., Kaur, T., Thakur, I., Verma, A., Wanchoo, R. K., & Toor, A. P. (2022). Photocatalytic degradation of pesticide monocrotophos in water using W-TiO2 in slurry and fixed bed recirculating reactor. *Journal of Molecular Structure*, *1265*, 133392. https://doi.org/10.1016/J.MOLSTRUC.2022.133392

Vijgen, J., Weber, R., Lichtensteiger, W., & Schlumpf, M. (2018). The legacy of pesticides and POPs stockpiles—a threat to health and the environment. *Environmental Science and Pollution Research 2018 25:32*, *25*(32), 31793–31798. https://doi.org/10.1007/S11356-018-3188-3

Walker, E. K., Brock, G. N., Arvidson, R. S., & Johnson, R. M. (2022). Acute Toxicity of Fungicide–Insecticide–Adjuvant Combinations Applied to Almonds During Bloom on Adult Honey Bees. *Environmental Toxicology and Chemistry*, *41*(4), 1042–1053. https://doi.org/10.1002/ETC.5297

Zhao, G. P., Yang, F. W., Li, J. W., Xing, H. Z., Ren, F. Z., Pang, G. F., & Li, Y. X. (2020). Toxicities of Neonicotinoid-Containing Pesticide Mixtures on Nontarget Organisms. *Environmental Toxicology and Chemistry*, *39*(10), 1884–1893. https://doi.org/10.1002/ETC.4842

DOI: https//doi.org/10.22452/mjs.vol43no4.3
Malaysian Journal of Science 43(4): 20-30 (December 2024)